DOI 10.14622/Advances_48_2022_19

Generation of a paper embossing preview using 3D scanning and Fourier analysis

Jakob Feldmann[1], *Felix Braig*[1], *Dieter Spiehl*[1], *Edgar Dörsam*[1] *and Andreas Blaeser*[2,3]

[1] Technical University of Darmstadt, Department of Mechanical Engineering, Institute of Printing Science and Technology, Magdalenenstr. 2, 64289 Darmstadt, Germany

[2] Technical University of Darmstadt, Department of Mechanical and Process Engineering, Institute for BioMedical Printing Technology, Magdalenenstr. 2, 64289 Darmstadt, Germany

[3] Technical University of Darmstadt, Centre for Synthetic Biology, Schnittspahnstr. 10, 64287 Darmstadt, Germany

E-mails:feldmann@idd.tu-darmstadt.de;spiehl@idd.tu-darmstadt.de;doersam@idd.tu-darmstadt.de;blaeser@idd.tu-darmstadt.de

Short abstract

The design and manufacture of embossing tools is a strong bottleneck in the development of new embossed paper and cardboard products. In the previous conventional process, a new embossing tool often has to go through several iteration loops until a satisfactory embossing result is achieved with it in trial embossings. This not only causes considerable cost and time expenditure, but also delays the market launch of new products. In order to provide the possibility of a preliminary evaluation and preview of the embossing result, a method was developed to determine the embossing behavior in the desired substrate. For this purpose, a universal test tool is used to emboss the substrate to be embossed. The embossing result is then scanned in three dimensions. The two data sets, original heightmap and fitted 3D scan relief data, are then transformed into the frequency domain utilizing a fast Fourier transformation (FFT). With a comparison it can be determined which frequency ranges deviate by which amount between the original data and the real embossing result. This allows conclusions to be drawn about the embossing capability of details and embossing features, as well as the creation of a preview of future embossing reliefs for this substrate. The results of this approach are presented and their significance for the future design process of new embossing tools is discussed.

Keywords: embossing, 3D printing, additive manufacturing, heightmaps, Fourier transformation, structured light scanning

1. Introduction and background

In addition to graphic print, raised elements and embellishments on packaging are an important way of attracting the attention and recognition of a product for the end consumer market (Hartmann and Haupt, 2016). Next to a visual enhancement of features such as letters and logos, raised elements add a haptic component to the perception of packages. With increasing environmental awareness, more and more packaging that previously used plastic is being replaced by ones made of paper and cardboard (Burger, et al., 2021). While plastic blister packs can be vacuum formed into almost any shape, making it easy to create these elements, embossing must be used for raised features in paper packaging. Embossments in paper are also used for finishing of a wide range of other paper products, such as cards, advertising materials or as copy protection in documents (Werblow, 2009). In addition to purely decorative purposes, embossing can also serve to add functional elements, such as closure flaps, adhesive surfaces or hazard labels for the visually impaired (Wilken, 2013). Conventionally, a two-part embossing tool, consisting of a female die and a male die is used, which represent inversions of each other, to deform the substrate under the application of compressive force. In the process, the substrate is pressed by the male die into the cavity of the female die and conforms to its surface. After removal of the force the plastic deformation of the paper remains, leaving a permanent impression of the desired relief geometry on the substrate (Wilken, 2013).

Embossing tools used for paper embossing are commonly manufactured from metal blanks which are processed using CNC milling or even manual engraving (Fachverband deutscher Stanzformhersteller e.V., n.d.), which can be very time consuming and can take up to a full business day. The manufacturer of the embossing tool and the printshop that carries out the embossing are often two different entities. Hence, shipping and communication between companies prolong overall lead times further. In addition, an evaluation of the embossing relief is only possible after the production has been completed. Often, defects that need to be corrected and unsatisfactorily formed regions are discovered in the embossing result during initial embossing tests, so that the embossing tool has to be reworked or completely remanufactured. These, often necessary iterative design changes and long manufacturing duration per tool iteration result in lead times of up to several weeks from initial layout to the final embossing tool. Therefore, in contrast to digital graphical print, the preparation of a new embossment poses as an immense bottleneck in the conceptual design of a new packaging or other cardboard product. In addition, multiple iteration loops in the design of new embossing tools lead to a significant additional environmental impact. Each iteration consumes further resources, but most significantly requires transportation between manufacturer of the tool and the printshop. Feldmann, Spiehl and Dörsam (2021) presented a method to fabricate embossing dies directly from relief data using stereolithography additive manufacturing and presents a comparison of lead times between conventional and additive manufacturing. Although this approach enables production duration of approximately 2.5 hours per set of dies and therefore reducing the overall lead times and costs for a new embossing tool conception, the necessity for possible multiple iteration loops to match a desired embossing layout still remains. It becomes evident, that the reduction or elimination of necessary iteration steps would have an even larger impact on the reduction of the duration, cost and environmental impact of the whole process chain than only shortening production times per step.

We developed a basic method with which substrates can be characterized for embossing and a preview of the embossing result can be estimated. This allows visualization of the expected embossing result already during the initial design of the planned relief design, i.e. even before the production of the tool has started. The purpose of this work is to reduce the number of iterations required by identifying undesirable embossing results early in the embossing relief design process. Also, the preview could be used for communication, as one can get an idea of the intended result before the first test embossing.

2. Technology and methods

As a basic concept we designed a universal embossing test tool, which can be used to characterize substrates intended for embossments. Using this universal test tool, embossments are created which are then digitized using a structured-light 3D scanner. By comparing original data with the obtained 3D scan data of the embossing result, it can be determined which features of the relief design are attenuated by which amount through the embossing process. This is done by fast Fourier analysis (FFT) of the original and the scanned data, allowing the calculation of a comparing characteristic transfer function (CTF). The CTF describes the relative amount each frequency in the original embossing relief layout is altered due to the embossing process and can therefore be used to characterize the substrate and predict embossing results of future designs. The process steps are described in detail below.

2.1 Design of universal embossing test tool

The design of the universal embossing test tool has to fulfill several requirements in order to cover a wide range of possible embossing features and to be significant for an analysis in the Fourier representation. Ideally, the test relief contains features which result in a constant signal for every possible frequency in the Fourier transform, hence it should contain fine details which result in higher frequencies up to broader sections representing lower frequencies. Further, we want to analyze the anisotropic embossing feedback

of the substrate which can be achieved by orienting the lines and features in a circular shape. This also allows for a smooth transition of high frequency details from the center towards lower frequency details at the edge of the relief geometry, which facilitates avoidance of undesired spectral leakage by tapering the relief height at the edge towards zero. In addition to the elements that are used in the Fourier analysis, an individual marker is also placed at each of the four corners of the tool. These markers are imprinted during the embossing process onto the substrate and help to align the original data and 3D scan data with each other by means of feature detection and image matching (see section 2.4). The markers were designed to be as diverse as possible and to contain a variety of detectable features such as radii, edges and cusps, following suggestions discussed by Košťák and Slabý (2021) as well as to be well suited for embossing into a wide range of possible substrates. Also, their positioning in the corners of the tool and thus at maximum distance from each other ensure that the transformation following image matching via homography (Hartley and Zisserman, 2004) can be as accurate as possible. Larger distances between markers ensure that only negligible angular error is induced for small lateral deviations when matching features. Figure 1 shows an 8-bit heightmap representation of the relief geometry of the universal embossing test tool of 2 000 × 2 000 pixels, as it was also used to create the test tool using additive manufacturing, as well as a rendered relief derived from it. Heightmaps represent the elevation of each point of the surface by the brightness of each pixel.

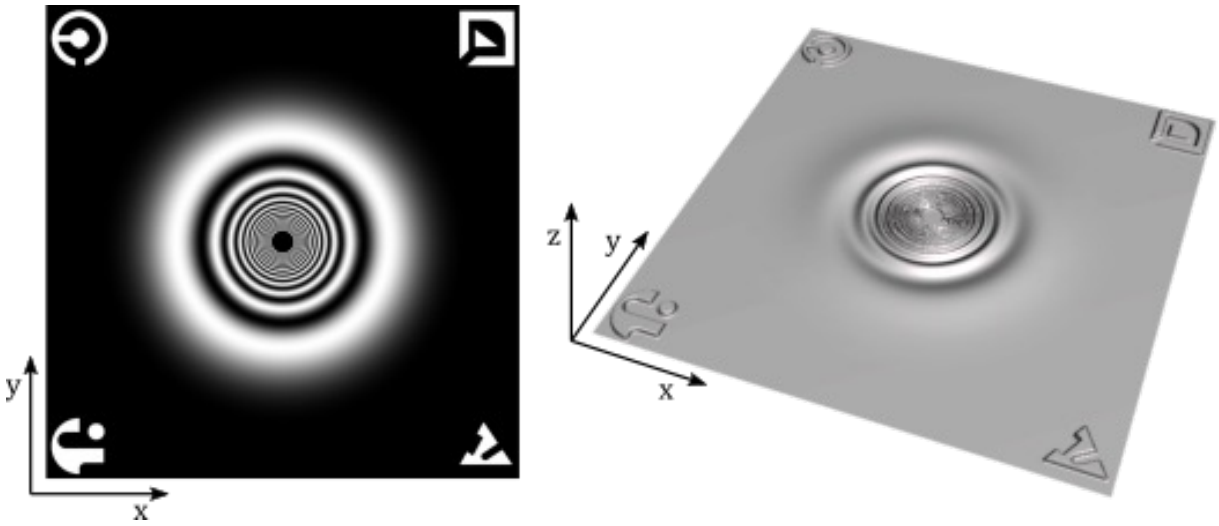

Figure 1: 8-bit heightmap of the universal test tool relief design on the left and derived rendered surface of it on the right; concentric rings with features that become narrower towards the center ensure the greatest possible coverage of the frequency spectrum, the ring-shaped arrangement also allows for analysis of embossing features in all possible orientations, and the four elements in the corners of the relief serve as markers for later feature detection and homographic matching between original data and 3D scanned data

2.2 Additive manufacturing of universal embossing test tool

Following the workflow presented by Feldmann, Spiehl and Dörsam (2021), a masked stereolithography (MSLA) additive manufacturing system (*Sharebot Viking*, Sharebot, Italy) was used for the fabrication of all embossing tools. The MSLA machine features a liquid crystal display with a resolution of 2 560 × 1 600 pixels and with a screen size of 182 mm × 120 mm, resulting in a lateral pixel resolution of 75 µm. The layer height was set to 25 µm, which is the minimum the machine can achieve. All embossing tools were fabricated with commercially available resin (*Azure Blue Tough Resin*, Prusa Research, Czech Republic). Adhesion to the build platform was increased by printing the first 8 layers of each tool with higher exposure time of 55 seconds per layer. All other layers were exposed for 5.5 seconds to UV-light during the fabrication process. After printing all tools were rinsed in isopropyl alcohol for at least 15 minutes to remove uncured resin residue, dried and post-treated in an UV-curing chamber (*Form Cure*, Formlabs, USA) for 15 minutes

at 40 °C. The tool is set to be of a size of 55 × 55 mm with a maximum embossing depth of 0.5 mm and a tool gap of 0.1 mm between fully closed female and male die. For the male embossing die the relief was printed via MSLA directly onto a bi-directional reinforced fiberglass composite sheet of a thickness of 0.5 mm, which was attached on the printing platform using adhesive tape. A fiberglass panel was chosen, which is made with epoxy resin to favor the best possible bond between it and the chemically similar additive manufacturing resin. This allows for the male die to be very thin, thus application on a wide range of embossing machines can be realized, even where space for male dies is limited. Both tool dies of the universal embossing tool are shown in Figure 2.

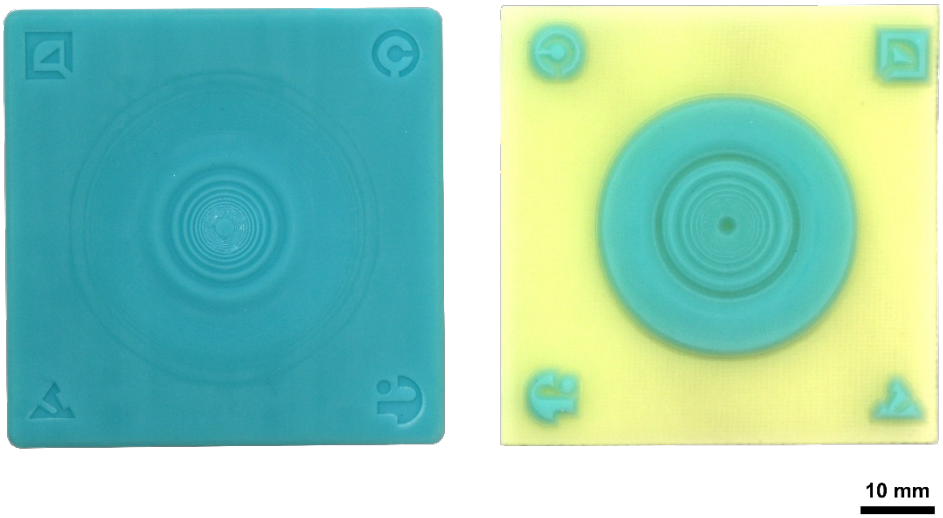

Figure 2: Photograph of the universal embossing test tool, the female die is displayed on the left and the male die on the right; while the female die was entirely additively manufactured using MSLA stereolithography, the embossing relief of the male die was printed via MSLA onto a sheet of fiberglass

2.3 Embossing and 3D scan examination

For the creation of embossments for examination via 3D scanning, a cotton substrate was selected that is common for embossing products (*Gmund Cotton* 450 g/m^2, Büttenpapierfabrik Gmund GmbH & Co. KG, Germany), which was embossed on an embossing press (*Geba 6*, Baier, Germany) under a load of 10 kN. Samples were then cut to approximate size and scanned using an optical 3D profilometer (*Keyence VR 5200*, Keyence, Japan), which achieves a lateral resolution of 23.53 µm using 12× optical magnification. The 3D scanning system is based on structured light, in which a known light pattern is projected onto the 3D object. Based on the deformation of the light pattern, which is recorded by a camera, the 3D surface of the object can then be reconstructed (Bartol, et al., 2021).

2.4 Data processing and analysis

The 3D scan is output in the form of two-dimensional data arrays, which contain the respective height of the embossment as a value in a grid with a lateral resolution of 23.53 µm. This results in a 2D data array of approximately 2 300 × 2 300 data points for the relevant area of the embossing relief, which has a size of 55 mm × 55 mm (see section 2.2). In a first step, the 3D scan data is transformed using a homography transformation to align as closely as possible to the original heightmap. To accomplish this, the scan data itself is first converted into an 8-bit grayscale heightmap representation. Utilizing the Scale Invariant Feature Transform “SIFT” feature detection (Lowe, 2004) built into OpenCV 3.4.2 (Bradski, 2000), possible relevant features in the original heightmap and the 3D scan data are identified and collected. Image features are then compared between the original and the scan heightmaps and closest matches are listed employing the Fast Library for Approximate Nearest Neighbors “FLANN” (OpenCV team, 2022). These

feature matches can then be used to find a homography transformation matrix (Hartley and Zisserman, 2004), which aligns the 3D scan onto the original heightmap, and therefore fits its resolution, orientation, distortion and lateral position. Although four feature matches are already sufficient for a fitting attempt, we found that applying the 10 closest feature matches gave the best results. The markers incorporated in the embossment design proved to be very beneficial for the performed image matching. Figure 3 shows a comparison between the original heightmap and the scan which was converted to a heightmap. Relevant features detected are highlighted in red, while the matches used for the homography transformation are shown as green lines between the two images.

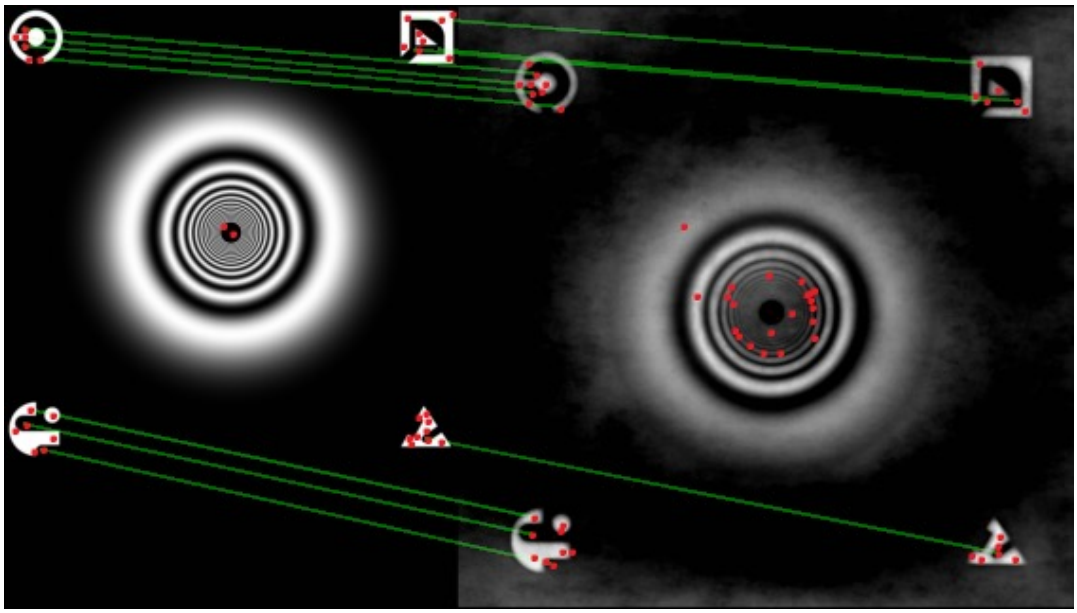

Figure 3: Visualization of found feature matches between the original heightmap used for the production of the embossing tool (left) and the 3D scanned and heightmap converted embossment (right); detected relevant features are shown as red dots, while the 10 most relevant matches are shown as green lines between the two images, note the importance of the matching markers in the corners of the embossing relief, which facilitate feature detection and matching

In a secondary step, the markers are cropped out, as they are no longer needed for the analysis once the two images are matched. The two data sets, original heightmap and fitted 3D scan relief data, are then transformed into the frequency domain utilizing a fast Fourier transformation (FFT). By comparing both transformed datasets we can obtain information about the embossment and the amount of alteration of features and their details depending on their size and orientation. For this, we calculate the characteristic transfer function (CTF) as the quotient for each data point *i,j* by dividing the Fourier transform of the 3D scanned data set $\mathcal{F}(HM_{\text{scan},i,j})$ by the Fourier transform of the original heightmap $\mathcal{F}(HM_{\text{original},i,j})$:

$$CTF_{i,j} = \frac{\mathcal{F}(HM_{\text{scan},i,j})}{\mathcal{F}(HM_{\text{original},i,j})} \quad [1]$$

We may now use this CTF to obtain an approximate preview of a future embossment, by elementwise multiplying the CTF to a Fourier transform of a new relief heightmap, provided that the new embossment is supposed to be done with the same compression force, a similar embossing depth and onto the same substrate.

$$\mathcal{F}\left(HM_{\text{preview},i,j}\right) = \mathcal{F}\left(HM_{\text{new},i,j}\right) \cdot CTF_{i,j} \quad [2]$$

Finally, we can view an estimated embossment preview by calculating an inverse Fourier transformation of the result of Equation [2].

2.5 Verification of the plausibility of the embossing preview

For verification of the here proposed model for approximation of embossments, another embossing tool was fabricated. In the same workflow as described in section 2.2 an embossing tool resembling a logo was created. This logo stands as an example of an embellishment, how it could be found on a cardboard box or other paper products. The heightmap depicting the logo used for the fabrication of this tool as well as the finished tool is shown in Figure 4. We took care to create it from a heightmap with the same resolution as the one used for the universal embossing test tool as well as setting its embossing depth to 0.5 mm and its tool gap to 0.1 mm, as it was done with the test tool. Also, the same embossing press, substrate and compression force was used. The physical embossment could then be 3D scanned and compared to the preview, obtained through the process outlined earlier.

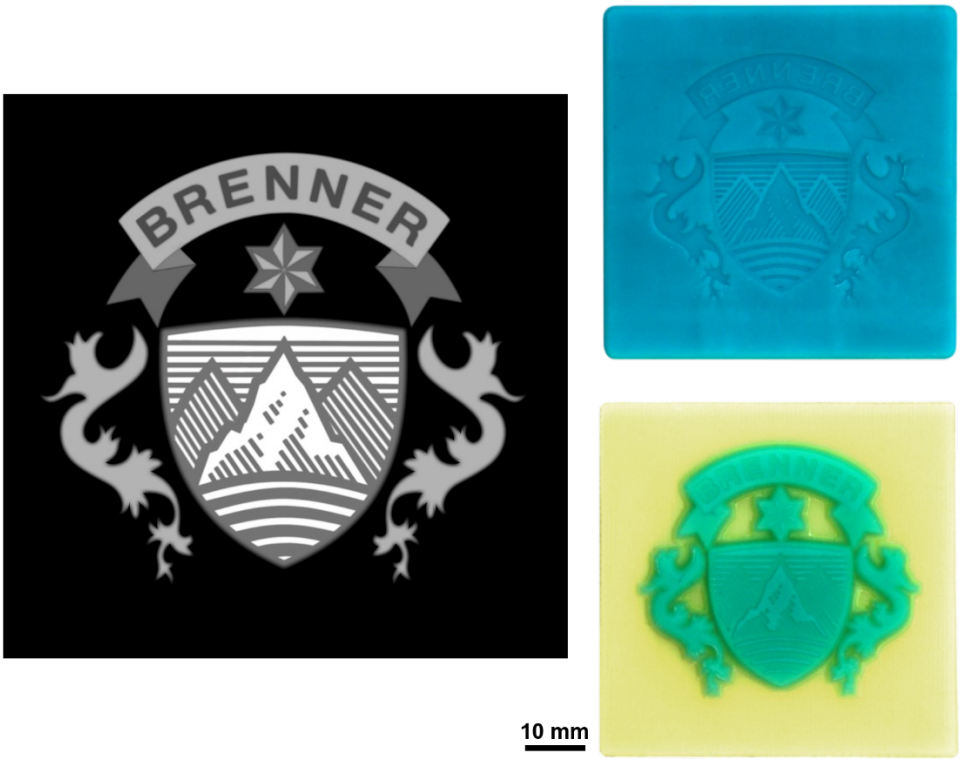

Figure 4: View of the 8-bit heightmap, on which the embossing tool to evaluate the plausibility of the embossing prediction is based (left) and an image of the embossing tool derived from it, consisting of a female die (top right) and a male die (bottom right)

3. Results and discussion

In initial tests of the algorithm, it could be shown that a comparison between the Fourier analysis of the original heightmap and the 3D scanned embossing result can indeed provide a rough indication of the characteristics of an embossing substrate and by which degree details are altered in the embossing process. An intuitive assessment of the attenuation of details by the embossing process is given by a polar display (Jähne, 2005) of the CTF, this is shown in Figure 5. Here, the transfer ratio for each orientation is displayed for each frequency. The recognizable wave structure of the CTF can possibly be explained by the finite resolution of the underlying data or the physical embossing tool. Likewise, the low number of quantification levels of an 8-bit heightmap may have an impact on the CTF's appearance. The influence of these factors or a combination of these are subject of future research.

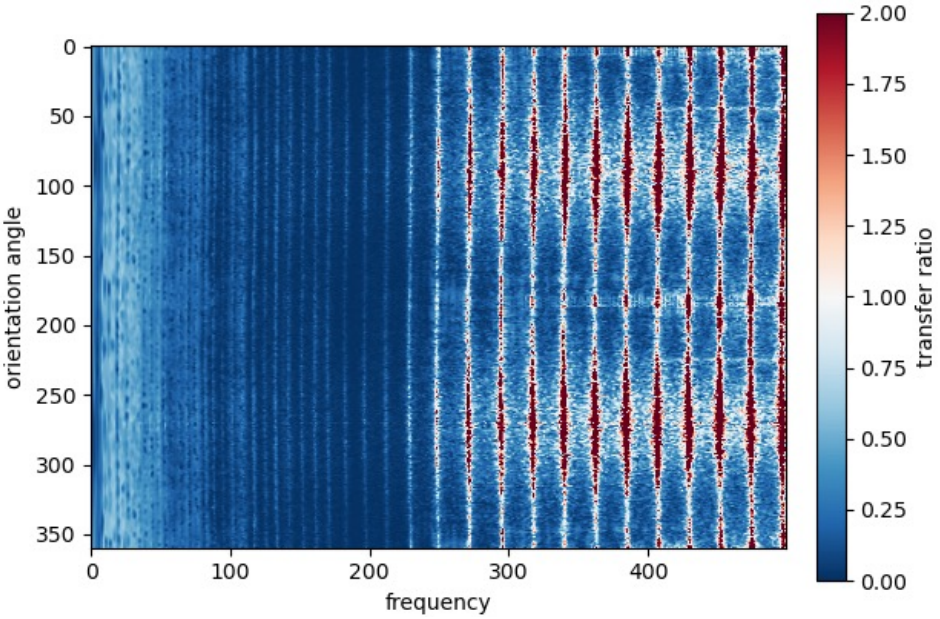

Figure 5: Representation of the characteristic transfer function (CTF) of the test embossment in polar coordinates (polar display); on the ordinate the angular orientation of the analyzed frequencies is plotted, while the frequency itself is displayed along the abscissa, the transfer ratio for each orientation and frequency is shown as either varying shades of blue for domains which are attenuated or red for domains, where the transfer ratio is greater than one, thus where an enhancement of the respective frequencies was found

To provide better access to the data shown in Figure 5, the transfer ratio can be averaged over all angles to show only the influence of the frequency on the transfer behavior. Thus, Figure 6 shows the average transfer ratio over all angles versus the frequency. For better visualization, the moving average was added in red, as well as a constant at a transfer ratio with the value one, representing the theoretical ideal embossment, where all details are fully transferred onto the substrate. It becomes apparent, that the amount of transfer changes depending on the frequency. Meaning, that the amount of transfer ratio (i.e. clarity or contrast of the embossment) changes according to the structure and details of the embossing relief. Since the physical feature size of these details can be calculated from the frequency if the size of the embossed image is known, a direct statement can be made about the transfer of individual features of the relief. Figure 7 therefore shows the transfer ratio versus the feature size of the embossing relief, which is equal to the inverse of the frequency, scaled according to the image size. Again, a constant at the transfer ratio with the value one was added, to visualize the theoretical ideal embossment transfer. For coarser embossing features, of 3 mm to 8 mm, the average transfer ratio reaches values of about 0.5, but shows significant reduction for smaller details. Below a feature size of approximately 0.5 mm the average transfer ratio rises significantly. This can be explained by the increased influence of the paper structure and paper fibers, which are in the domain of the 3D scan for small features, but are not included in the heightmap original.

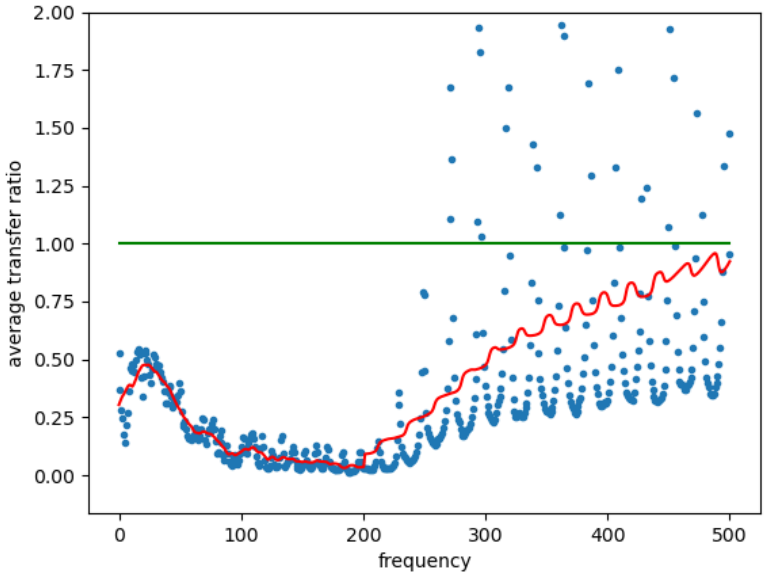

Figure 6: Representation of the average transfer ratio across all orientation angles; the red line represents the moving average of the frequency dependent transfer ratio, the green line visualizes the theoretical ideal transfer ratio with a constant value of one, if all details were impressed onto the substrate without deviation, note that larger frequency domains represent the transfer of smaller details and vice versa

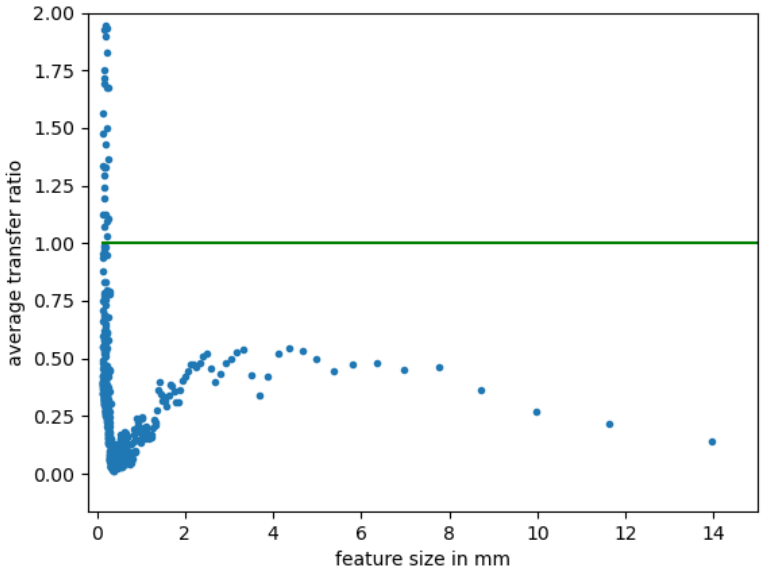

Figure 7: Representation of the average transfer ratio across all orientation angles plotted against the respective feature size of the transferred details, the green line visualizes the theoretical ideal transfer ratio with a constant value of one, if all details were impressed onto the substrate without deviation

Plotting the average transfer ratio per orientation angle and across all frequencies provides information about the dependence of the transfer of details and embossing features on their orientation in the embossing relief. In Figure 8, the average transfer ratio is plotted over all frequencies up to 250. The moving average is shown as a red line. It thus shows the angle-dependent transfer of details before the increase of the CTF, which is induced by the paper structure. It can be seen that the transfer of embossing details in the horizontal direction (90° or 270°) is higher than in the vertical direction (0° or 180°), which correlates with the cross direction (CD) of the substrate, which is also horizontal to the observer. These differences could have their origin in different mechanical properties of the substrate in machine and cross direction, which result in orthotropic embossing behavior (Kirwan, 2013) and the ductility of paper in CD is often significantly greater than in machine direction (MD) (Wilken, 2013).

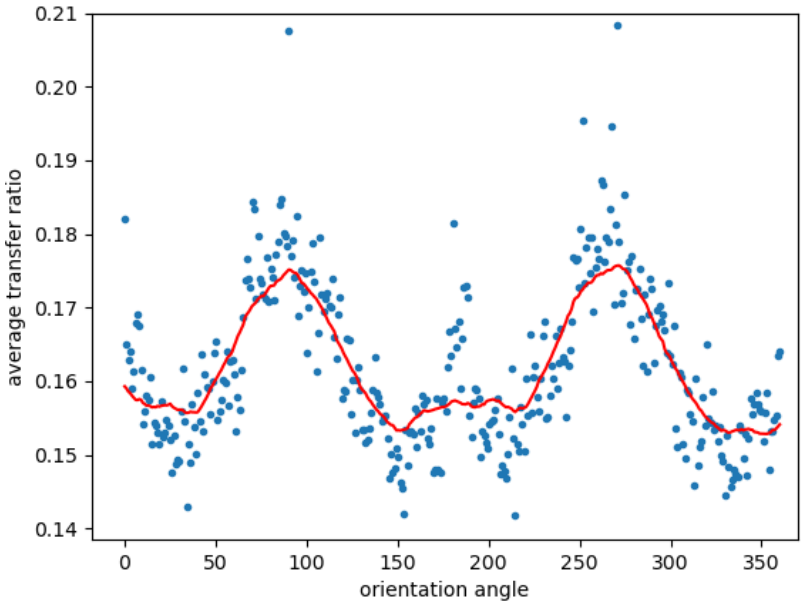

Figure 8: Plot of the average transfer ratio across all frequencies, thus visualizing alteration in transfer of details depending on orientation angle, an orthotropic behavior of the transfer can be identified, with larger transfer ratios along the 90° – 270° axis

The embossment preview obtained following Equation [2] shows satisfactory results. It delivers an estimation of the embossing result which can be expected by washing out details and attenuating sharp edges and corners of the relief design shown in Figure 4. Further, the impression of paper structure is added to the heightmap preview by increasing the grain of the image. Comparison between the preview and the 3D scan of the actual embossment, as shown in Figure 9, shows how close the outcome of the process described here matches the true embossing result.

Figure 9: Direct comparison of the estimated heightmap of the embossing preview and an actual 3D scanned embossment in cotton paper with a grammage of 450 g/m²

Figure 10 shows a representation of an embossing in white substrate, which was rendered on the basis of the preview heightmap, as well as a photograph of the real embossing in cotton paper with a grammage of 450 g/mm². Even though no perfect prediction is possible yet, the comparison demonstrates the potential of the approach to simulate and evaluate planned embossments in advance.

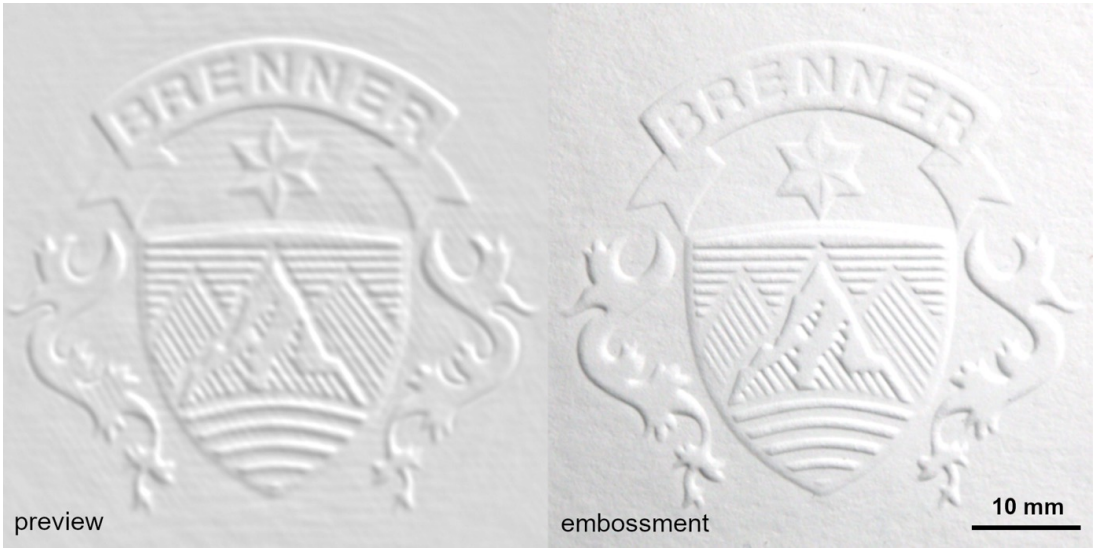

Figure 10: Comparison between a rendered visualization of the embossing preview, based on the heightmap shown in Figure 8 (left) and a photograph of the actual embossment, created with an embossing tool fabricated according to the same data under similar lighting conditions

4. Conclusions

The method presented in this text for characterizing embossing substrates, as well as the embossing previews generated by it, show potential to shorten the process chain and reducing the environmental impact of creating new embossing designs. It also forms a good basis for enabling further visualizations, for example for communication between designer, customer and manufacturer, which were previously only possible through time consuming and costly test embossing. Here, we have shown that the method is suitable for examining the entire process chain of creating a new embossment. Alternatively, it is conceivable to examine each intermediate step of the production process separately, which would reveal which sub process leads to which attenuations in the finished embossed image, e.g. which deviations are caused by the fabrication of the embossing tool and which by the embossing process itself. The algorithm forms the basis for an evaluation of the embossing behavior of different substrates, under different load conditions and environmental influences. Here, the workflow for a single substrate type was demonstrated. However, the test tool and algorithm can form a foundation for the creation of a database of various substrates. For systematic analyses, it can further be used as a tool for determining the influence of embossing parameters on the embossing result, so that in future more precise statements can be made in advance about the probable outcome of an embossing. Thus, not only the embossing relief design can be fit to the needs of the substrate, but also the right embossing parameters, such as compression force and humidity can be chosen accordingly. The generated analysis and preview so far shows the detail size-dependent deviation of the embossment, assuming that the embossing is in principle error-free. However, a frequent cause of necessary iteration loops in the design of new embossing tools are also artifacts and defects, such as tears, punch-outs or areas that were not completely impressed into the substrate. The object of future research is therefore the detection and evaluation of such defects, so that strategies can be developed to exclude or at least reduce them even before the first actual embossing is done. In addition, the approach shown here will be further developed and made into a generally applicable tool for characterizing embossing substrates. With its help embossing response of commonly used substrates will be collected and influences of different parameters on the embossment result will be analyzed.

References

Bartol, K., Bojanić, D., Petković, T. and Pribanić, T., 2021. A review of body measurement using 3D scanning. *IEEE Access*, 9, pp. 67281–67301. http://doi.org/10.1109/ACCESS.2021.3076595.

Bradski, G., 2000. The OpenCV library. *Dr. Dobb's Journal*, 25(11), pp. 120–126.

Burger, A., Cayé, N., Jaegermann, C. and Schuler, K., 2021. *Aufkommen und Verwertung von Verpackungsabfällen in Deutschland im Jahr 2019: Abschlussbericht*. Mainz: GVM Gesellschaft für Verpackungsmarkforschung mbH, im Auftrag des Umwelt Bundesamt.

Fachverband deutscher Stanzformhersteller e.V., n.d. Esupedia: *Stanzwerkzeuge für die Karton- und Wellpappenverarbeitung.* Meerbusch, Germany: Europäische Stanzform Union e.V.

Feldmann, J., Spiehl, D., and Dörsam, E., 2021. Paper embossing tools: a fast fabrication workflow using image processing and stereolithography additive manufacturing. In: C. Ridgway, ed. *Advances in Printing and Media Technology: Proceedings of the 47th International Research Conference of iarigai*. Athens, Greece, 19–23 September 2021. Damstadt: iarigai, pp. 146–154. http://dx.doi.org/10.14622/Advances_47_2021.

Hartley, R. and Zisserman, A., 2004. *Multiple view geometry in computer vision*. 2nd ed. Cambridge: Cambridge University Press.

Hartmann, O. and Haupt, S., 2016. *Touch!: Der Haptik-Effekt im multisensorischen Marketing*. 2nd ed. Freiburg, München, Stuttgart: Haufe Gruppe.

Jähne, B., 2005. *Digital image processing*. 6th ed. Berlin, Heidelberg, New York: Springer.

Kirwan, M.J. ed., 2013. *Handbook of paper and paperboard packaging technology*. 2nd ed. Chichester, West Sussex: Wiley-Blackwell.

Košťák, M. and Slabý, A., 2021. Designing a simple fiducial marker for localization in spatial scenes using neural networks. *Sensors*, 21(16): 5407. http://doi.org/DOI: 10.3390/s21165407.

Lowe, D., 2004. Distinctive image features from scale-invariant keypoints. *International Journal of Computer Vision*, 60(2), pp. 91–110. https://doi.org/10.1023/B:VISI.0000029664.99615.94.

OpenCV team, 2022. *FLANN: Fast library for approximate nearest neighbors.* [online] Available from: <https://docs.opencv.org/3.4.2/dc/de2/classcv_1_1FlannBasedMatcher.html> [Accessed 18 April 2022].

Werblow, S., 2009. Anti-counterfeiting packaging. In: K.L. Yam, ed. *The Wiley encyclopedia of packaging technology*. 3rd ed. Hoboken: John Wiley & Sons, pp. 46–48.

Wilken, R., 2013. Verfahren der Papierbearbeitung. In: J. Blechschmidt, ed. *Papierverarbeitungstechnik*. München: Fachbuchverl. München: Carl Hanser Verlag, pp. 130–241.